Chapter 12
Variable Thrust Angle Constant Thrust Rendezvous

Yongqiang Qi and Ding Lv

Abstract In this paper, variable thrust angle (VTA) constant thrust rendezvous is studied. In particular, the rendezvous process is divided into in-plane motion and out-plane motion based on the relative motion dynamic model. For the in-plane motion, the calculation of thrust angle control lows is cast into a convex optimization problem by introducing a Lyapunov function subject to linear matrix inequalities. For the out-plane motion, a new algorithm of constant thrust fitting is proposed through the impulse compensation. The illustrative example is provided to show the effectiveness of the proposed control design method.

Keywords Rendezvous · Constant thrust · Variable thrust angle · Robust controller

12.1 Introduction

The problem of rendezvous has been studied and many results have been reported. For example, the optimal impulsive control method for rendezvous is studied in [1]; adaptive control theory is applied to the rendezvous problem in [2]; an annealing algorithm method for rendezvous orbital control is proposed in [3]; maneuvers during rendezvous operations cannot normally be considered as continuous thrust maneuver or impulsive maneuver [4–6]. In addition, the variable thrust angle (VTA) constant thrust maneuver, until recent years, has been the least studied.

The purpose of this paper is to study VTA constant thrust rendezvous, in other words, to design robust closed-loop VTA control laws for the in-plane motion, and to calculate and compare the fuel consumption under the theoretical continuous thrust and the actual constant thrust. First of all, for in-plane motion, the robust control laws for constant thrust VTA satisfying the requirements can be designed by

Y. Qi (✉) · D. Lv
College of Sciences, China University of Mining and Technology (CUMT), Xvzhou, China
e-mail: qiyongqiang3@163.com

Z. Deng and H. Li (eds.), *Proceedings of the 2015 Chinese Intelligent Automation Conference*, Lecture Notes in Electrical Engineering 337,
DOI 10.1007/978-3-662-46463-2_12

solving the convex optimization problem. Then, for out-plane motion, a new algorithm of constant thrust fitting is proposed by using the impulse compensation method. Finally, the optimal fuel consumption can be obtained by comparing the theoretical thrust and the actual constant thrust, and then the actual working times of the thrusters can be computed using time series analysis method. An illustrative example shows the effectiveness of the proposed control design method.

12.2 The Robust Variable Thrust Angle Control Laws for In-plane Motion

The relative motion coordinate system can be established as follows: first, the target spacecraft is assumed as a rigid body and in a circular orbit, and the relative motion can be described by Clohessy-Wiltshire equations. Then, the centroid of the target spacecraft O_T is selected as the origin of coordinate, the x-axis is opposite to the target spacecraft motion, the y-axis is from the center of the earth to the target spacecraft, the z-axis is determined by the right-handed rule. Then the collision avoidance process can be divided into in-plane motion and out-plane motion based on the relative motion dynamic model as follows, where the relative motion dynamic model of the in-plane motion is:

$$\begin{cases} \ddot{x} - 2\omega\dot{y} = \frac{F_x + \eta_x}{m} \\ \ddot{y} + 2\omega\dot{x} - 3\omega^2 y = \frac{F_y + \eta_y}{m} \end{cases} \tag{12.1}$$

where ω represents the angular velocity of the target spacecraft. F_x, F_y represent the vacuum thrust of the chaser and η_x, η_y represent the sum of the perturbation and nonlinear factors in the x-axis and in the y-axis, respectively. m represents the mass of the chaser at the beginning of the collision avoidance maneuver.

Suppose the actual constant thrusts of the chaser are F_x, F_y, F_z, the maximum thrusts are $\widehat{F}_x, \widehat{F}_y, \widehat{F}_z$, and the theoretical continuous thrusts are F_x^*, F_y^*, F_z^*.The range of the thrust angle in the x-axis θ_x is defined as shown in Figs. 12.1.

The goal of the collision avoidance maneuver is to design a proper controller for the chaser, such that the chaser can be asymptotically maneuvered to the target position. Define the state error vector $x_e(t) = x(t) - x_t(t)$, and its state equation can be obtained as

$$\begin{cases} \dot{x}_e(t) = (A_1 + \Delta A)x_e(t) + (B_1 + \Delta B)u(t) \\ u(t) = Kx_e(t) \end{cases} \tag{12.2}$$

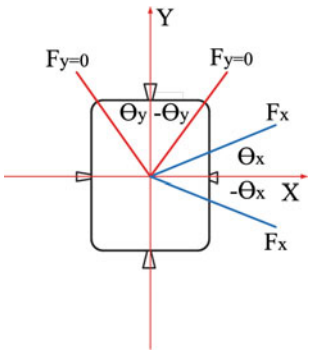

Fig. 12.1 Variable thrust angle thrusters

Lyapunov function is defined as follows:

$$V = x_e^T(t)Px_e(t) \tag{12.3}$$

where P is a positive definite symmetric matrix. According to the system stability theory, the necessary and sufficient conditions for robust stability of the system (12.2) are as follow:

$$A^T P + PA < 0 \tag{12.4}$$

Then a multi-objective controller design strategy is proposed by translating a multi-objective controller design problem into a convex optimization problem. And the control input constraints can be met simultaneously. Assuming the initial conditions satisfy the following inequality, where ρ is a given positive constant.

$$x^T(0)Px(0) < \rho \tag{12.5}$$

Theorem 12.1 *If there exist a corresponding dimension of the matrix L, a symmetric positive definite matrix X and two parameters* $\varepsilon_1 > 0, \varepsilon_2 > 0$, *then for sufficient condition for robust stability there exist a state feedback controller K which can meet the following conditions simultaneously*:

$$\begin{pmatrix} \Sigma & X & L \\ X & -\varepsilon_1 & 0 \\ L^T & 0 & -\varepsilon_2 \end{pmatrix} < 0, \qquad \begin{pmatrix} \rho I & x^T(0) \\ x(0) & X \end{pmatrix} < 0, \tag{12.6}$$

where $\Sigma = XA_0^T + A_0X + L^TB_0 + B_0L + \varepsilon_1\alpha^2 I + \varepsilon_2\beta^2 I$, *then the theoretical state feedback controller K can be calculated as follows*:

$$K = LX^{-1} = \begin{pmatrix} K_{11} & K_{12} & K_{13} & K_{14} \\ K_{21} & K_{22} & K_{23} & K_{24} \end{pmatrix} \tag{12.7}$$

Then the following results can be obtained:

$$\begin{cases} \dfrac{L_x}{N_x}\hat{F}_x \cos\theta_x + \dfrac{L_y}{N_y}\hat{F}_y \sin\theta_y = k_{11}x_e(t) + k_{12}y_e(t) + k_{13}\Delta V_x + k_{14}\Delta V_y \\ \dfrac{L_x}{N_x}\hat{F}_x \sin\theta_x + \dfrac{L_y}{N_y}\hat{F}_y \cos\theta_y = k_{21}x_e(t) + k_{22}y_e(t) + k_{23}\Delta V_x + k_{24}\Delta V_y \end{cases} \tag{12.8}$$

Then the thrust angle control lows θ_x, θ_y which satisfy the robust stability of the in plane motion can be obtained from Eq. (12.8).

12.3 Compare Fuel Consumption for the Out-plane and Calculate the Control Law

The relative motion dynamic model of the out-plane motion:

$$\ddot{z} + \omega^2 z = \frac{F_z + \eta_z}{m} \tag{12.9}$$

For the out-plane motion, a new algorithm of constant thrust fitting is proposed using the impulse compensation method as follows. Suppose the thrusters in the z-axis can provide different sizes of constant thrust to meet different thrust requirements.

Constant thrust fitting is proposed by using the impulse compensation method as follows. Suppose the thrusters in the z-axis can provide different sizes of constant thrust to meet different thrust requirements. If the theoretical working time of z-axis thruster in the ith thrust arc $t_z^* = \Delta T < T_i$ and t_z^* can be any one of M_i shortest switching time interval in the ith thrust arc. Without loss of generality, suppose t_z^* is the first shortest switching time interval and the impulse error in the z-axis in the ith thrust arc ΔI_{zi} can be calculated as follows:

There are $N_z + 1$ thrust levels that can be selected and the level of the constant thrust can be calculated as follows:

$$L_z = \left[\frac{N_z \int_{T_i}^{T_i + \Delta T} \left| F_z^*(t) \right| \mathrm{d}t}{\hat{F}_z \Delta T} \right] \tag{12.10}$$

Calculate the impulse error.

$$\Delta I_{zi} = \operatorname{sgn}\left(F_z^*(t)\right)\left|\int_{T_i}^{T_{ii}+\Delta T}\left|F_x^*(t)\right|\mathrm{dt} - \frac{L_z\hat{F}_z\Delta T}{N_z}\right| \tag{12.11}$$

Determine the value of the impulse compensation threshold. Suppose the value of the impulse compensation threshold is a positive constant $\gamma > 0$, if the impulse error ΔI_{zi} satisfies the following condition:

$$\left|\int_{T_i}^{T_{ii}+\Delta T}\left|F_x^*(t)\right|dt - \frac{\hat{F}_z\Delta T}{N_z}\left[\frac{N_z\int_{T_i}^{T_i+\Delta T}\left|F_z^*(t)\right|}{\hat{F}_z\Delta T}\right]\right| \le \gamma \tag{12.12}$$

the actual constant thrust of the chaser in the z-axis can be calculated as follows:

$$F_z = \operatorname{sgn}(F_z^*(t))\frac{\hat{F}_z\Delta T}{N_z}\left[\frac{N_z\int_{T_i}^{T+\Delta T_i}\left|\hat{F}_z^*(t)\right|dt}{\hat{F}_z\Delta T}\right] \tag{12.13}$$

then the chaser will not carry out impulse compensation. Suppose

$$\left[\left|\int_{T_i}^{T_i+M_1\Delta T}\frac{F_z^*(t)N_z}{\hat{F}_z\Delta T}\mathrm{dt} - \int_{\mathrm{T_1}+(\mathrm{m_1}+1)\Delta\mathrm{T}}^{\mathrm{T_i}+\mathrm{M_1}\Delta\mathrm{T}}\{\frac{\operatorname{sgn}(\mathrm{F_z^*(t)})}{\Delta\mathrm{T}}\left[\frac{\mathrm{N_z}\int_{\mathrm{T_i}+\mathrm{j}\Delta\mathrm{T}}^{\mathrm{T_i}+(\mathrm{j}+1)\Delta\mathrm{T}}\left|\mathrm{F_z^*(t)dt}\right|}{\hat{\mathrm{F}}_\mathrm{z}\Delta\mathrm{T}}\right]\}\mathrm{dt}\right|\right] = m_2 \tag{12.14}$$

Furthermore, if the impulse error ΔI_{zi} satisfies the following condition:

$$\left[\left|\int_{T_i}^{T_i+M_1\Delta T}F_z^*(t)\mathrm{dt} - \int_{\mathrm{T_1}+(\mathrm{m_1}+1)\Delta\mathrm{T}}^{\mathrm{T_i}+\mathrm{M_1}\Delta\mathrm{T}}\{\operatorname{sgn}(\mathrm{F_z^*(t)})\frac{\hat{\mathrm{F}}_\mathrm{z}}{\mathrm{N_z}}\left[\frac{\mathrm{N_z}\int_{\mathrm{T_i}+\mathrm{j}\Delta\mathrm{T}}^{\mathrm{T_i}+(\mathrm{j}+1)\Delta\mathrm{T}}\left|\mathrm{F_z^*(t)dt}\right|}{\hat{\mathrm{F}}_\mathrm{z}\Delta\mathrm{T}}\right]\}\mathrm{dt}\right|\right] < \gamma \tag{12.15}$$

if the impulse error ΔI_{zi} satisfies the following condition:

$$\left[\left|\int_{T_i}^{T_i+M_1\Delta T}F_z^*(t)\mathrm{dt} - \int_{\mathrm{T_1}+(\mathrm{m_1}+1)\Delta\mathrm{T}}^{\mathrm{T_i}+\mathrm{M_1}\Delta\mathrm{T}}\{\operatorname{sgn}(\mathrm{F_z^*(t)})\frac{\hat{\mathrm{F}}_\mathrm{z}}{\mathrm{N_z}}\left[\frac{\mathrm{N_z}\int_{\mathrm{T_i}+\mathrm{j}\Delta\mathrm{T}}^{\mathrm{T_i}+(\mathrm{j}+1)\Delta\mathrm{T}}\left|\mathrm{F_z^*(t)dt}\right|}{\hat{\mathrm{F}}_\mathrm{z}\Delta\mathrm{T}}\right]\}\mathrm{dt}\right|\right] > \gamma \tag{12.16}$$

then the chaser should carry out impulse compensation and the size of the constant thrust impulse compensation in the z-axis can be calculated as follows:

$$\begin{aligned}\Delta I_{zi} &= F_5 m_2 \Delta T = \frac{m_2 \hat{F}_z \Delta T}{N_z}, (F_z^*(t) < 0) \\ \Delta I_{zi} &= F_6 m_2 \Delta T = -\frac{m_2 \hat{F}_z \Delta T}{N_z}, (F_z^*(t) > 0)\end{aligned} \tag{12.17}$$

the actual constant thrust of the chaser in the x-axis can be calculated as follows. The fuel savings in the x-axis in the ith thrust arc can be calculated as follows:

$$\Delta P_{zi} = \sum_{j=0}^{M_1} \int_{T_i + j\Delta T}^{T_i + (j+1)\Delta T} \left\{ \frac{p_0 N_z \left| F_z^*(t) \right|}{\hat{F}_z} - \mathrm{sgn}(F_z^*(t)) p_0 \left[\frac{N_z \int_{T_i + j\Delta T}^{T + (j+1)\Delta T} \left| \hat{F}_z^*(t) \right| dt}{\hat{F}_z \Delta T} \right] \right\} dt \tag{12.18}$$

Finally, the switch control laws for the rendezvous maneuver can be given in three axes. For convenience, let us take the time intervals in the ith thrust arc in the x-axis for example:

$$S_{zi} = \left\{ \left(T_i + j\Delta T, \mathrm{sgn}(F_z^*(t)) \frac{\hat{F}_z \Delta T}{N_z} \left[\frac{N_z \int_{T_i + j\Delta T}^{T + (j+1)\Delta T} \left| \hat{F}_z^*(t) \right| dt}{\hat{F}_z \Delta T} \right] \right) \right\} \tag{12.19}$$

12.4 Simulation Example

The height of target spacecraft is assumed to be 356 km in a circular orbit, then the mean angular velocity is $\omega = 0.0654 \times 10^{-3}\mathrm{rad/s}$ and the uncertainty parameters is assumed as $\Delta\omega = \pm 1 \times 10^{-3}\mathrm{rad/s}$. The initial mass of the chaser is assumed to be 180 kg at the beginning of rendezvous maneuver. The size of thrusts are assumed to be $\pm 1{,}200\,\mathrm{N}$ in three axes and the shortest switching time is $\Delta T = 1\mathrm{s}$ The initial position and velocity of the chaser are assumed to be (1000, 500, −200 m) and (−10; −5; 2 m/s).

Figure 12.2 shows the change in x, y, z and V_x, V_y, V_z during rendezvous maneuver.

The results in Fig. 12.3 show the change in F_x, F_y, F_z during rendezvous maneuver.

The result in Fig. 12.4 shows the trajectory of chaser and the change of the thrust angles during rendezvous maneuver. It shows that with the switch control control, the chaser can get to the 20 target positions smoothly.

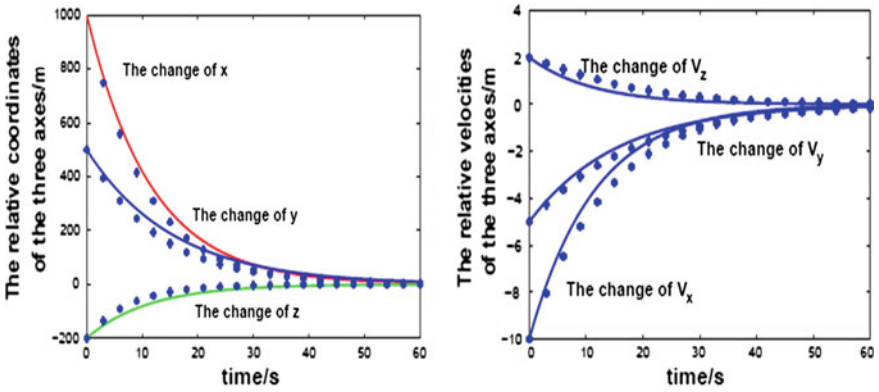

Fig. 12.2 The change of position and velocity during rendezvous maneuver

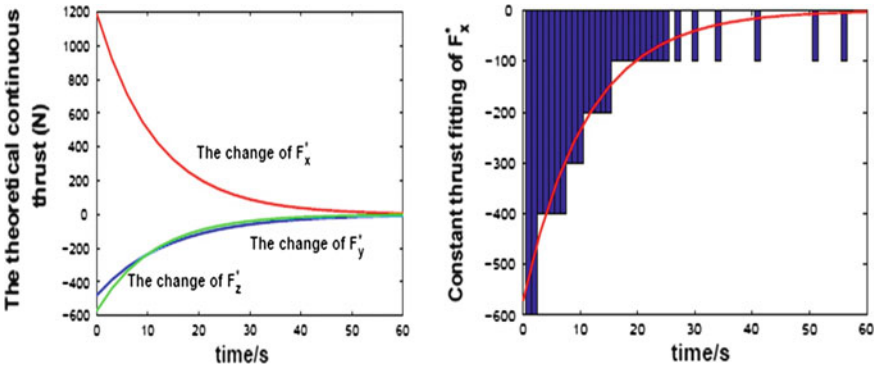

Fig. 12.3 The change of thrust during rendezvous maneuver

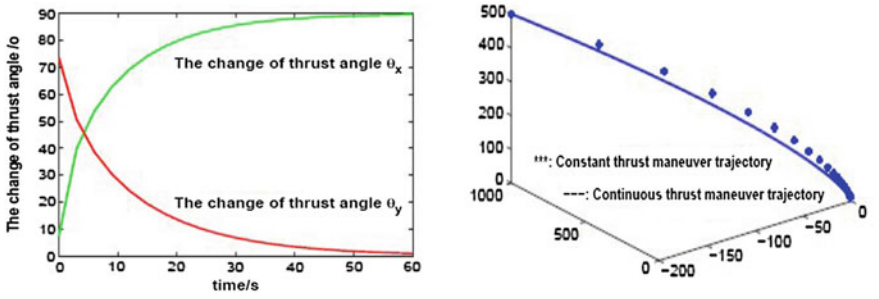

Fig. 12.4 The change in the trajectory of the chaser and thrust angles

The switch control laws can be given according to the sizes and the directions of the thrust of the chaser. Taking the switch control law in the z-axis as an example:

$$S_{zi} = \{(\Delta T, -600); \ldots; (27\Delta T, -100); \ldots; (30\Delta T, 0)\} \tag{12.20}$$

Acknowledgments This work was supported by the NSFC 61304088 and 2013QNA37.

References

1. Jezewski DJ, Donaldson JD (1979) An analytical approach to optimal rendezvous using Clohessy-Wiltshire equations. J Astronaut Sci 27(3):293–310
2. Slater GL, Byram SM, Williams TW (2006) Rendezvous for satellites in formation flight. J Guidance Control Dyn 29:1140–1146
3. Ebrahimi B, Bahrami M, Roshanian J (2008) Optimal sliding-mode guidance with terminal velocity constraint for fixed-interval propulsive maneuvers. Acta Astronaut 60(10):556–562
4. Schouwenaars T, How JP, Feron E (2004) Decentralized cooperative trajectory planning of multiple aircraft with hard safety guarantees. In: AIAA paper, 2004
5. Richards A, Schouwenaars T, How J et al (2002) Spacecraft trajectory planning with avoidance constraints using mixed integer linear programming. J Guidance Control Dyn 25(4):755–764
6. Qi YQ, Jia YM (2012) Constant thrust fuel-optimal control for spacecraft rendezvous. Adv Space Res 49(7):1140–1150